

Behavior of the correlation range in a gravitational field

A. D. Alekhin

Kiev State University

(Submitted July 9, 1976)

Zh. Eksp. Teor. Fiz. 72, 1880–1884 (May 1977)

The effect of gravity on the behavior of the correlation range of simple substances and binary solutions near the critical state of vaporization is investigated on the basis of experimental data on the integral intensity of the scattered light. Asymptotic power laws for the behavior of the correlation range along a critical isochor, a phase boundary, and a critical isotherm are investigated.

PACS numbers: 64.60.Ht

The experimental study of second-order phase transitions and of critical phenomena is basically aimed at the elucidation of the character of the singularities in the thermodynamic properties of a system. The studies of the causes of these singularities, i. e., of the correlation properties of a substance, are very few in number. The main information in this direction is given by experiments on the scattering of visible and x-ray radiation.^[1] There, the authors limit themselves to the study of the temperature dependence of the correlation range along a critical isochor or phase boundary.

For a more thorough characterization of the properties of a medium in the near-critical state, field investigations of the correlation properties of a substance are also very necessary. A very convenient subject for experiments of a similar nature are systems in the earth's gravitational field near the critical state of vaporization. The necessary conditions for field investigations of the correlation range are realized owing to the unlimited increase in the susceptibility of such systems to the slightest external effects.

In the present work, the gravitational effect is used for the study of the field and temperature dependences of the correlation range near the critical state of vaporization in three substances: in a simple paraffin—*n*-pentane and in two solutions of 26.8 and 38.3 mol. % benzene in *n*-pentane.

The investigations were carried out with experimental apparatus^[2] which allows the study of the height distribution of the extinction coefficient and of the integral intensity of scattered light at an angle of 90°. Corrections were introduced into the experimental data on the scattering intensity to take into account the attenuation of the incident and scattered light fluxes and also the contribution of secondary scattering. The method of introducing these corrections, and their absolute values both far from the critical state and near it, are discussed in detail in^[3, 4]. Calculations show^[4] that the fraction of secondary scattering in the total flux of scattered light varies from 1 to 15% at $\lambda = 5461 \text{ \AA}$, depending upon the height H and temperature $t = (T - T_{cr})/T_{cr}$. This comparatively small contribution of the secondary scattering is connected with the strong inhomogeneity of the extinction coefficient as a function of the height of the system.^[5] The overall error in the thus obtained single-scattering intensity varies from 2 to 6%, depending upon the height H and the temperature t . The indicated

errors consist of the random errors caused by the noise of the electronic devices (1–2%), and of the errors resulting from corrections for the attenuation of the incident and scattered light fluxes and for secondary scattering (1–4%), which have a systematic character within the limits of one isotherm $I(H, t)$ of the light-scattering intensity.

The filling of the chamber with material was carried out in such a way that at the critical temperature T_{cr} the meniscus separating the liquid and the gaseous phases disappeared in the middle of the chamber. In the region of temperatures $T > T_{cr}$, the level $H=0$ corresponds to the maximum of the gradient of the concentration density and consequently of the intensity of the scattered light. At this height and at $T > T_{cr}$, the critical values of the density and of the concentration are realized under the influence of the gravitational field. When the temperature changes in the transcritical region, the height of this maximum in the container remained practically constant. At temperatures below the critical value the level $H=0$ corresponds to a phase boundary in both pure substances and in binary solutions. At heights $H < 0$, we have $\rho > \rho_{cr}$, while at $H > 0$ the density $\rho < \rho_{cr}$. The critical temperature was taken to be the one at which the intensity of the scattered light at the height $H=0$ was a maximum. For *n*-pentane, $T_{1cr} = 469.98 \text{ K}$, and for the solutions 26.8 and 38.3% benzene in *n*-pentane $T_{2cr} = 490.09 \text{ K}$ and $T_{3cr} = 498.86 \text{ K}$, respectively. Near the critical temperature, the substance was maintained at constant temperature for 10 to 12 hours accurate to 0.005°. The height distributions of the intensity of single scattering at the critical temperatures of the substances studied were used to investigate the field dependence of the correlation range.

The behavior of the intensity of single scattering at the height $H=0$ and at $T > T_{cr}$ was used to study the temperature dependence of the correlation range along a critical isochor, and at $T < T_{cr}$ —along a phase boundary. During the measurement of the intensity of the scattered light at the height $H=0$ in the temperature range $T < T_{cr}$, the radiation incident on the photomultiplier comes from a layer of matter 0.6 mm thick, containing liquid and gaseous phases. As experimental investigations have shown,^[5] near the critical point, owing to the influence of the gravitational field, the slightest departure in height from the level $H=0$ in the direction of the liquid or of the gaseous phase leads to a

sharp reduction in the intensity of the light scattering. Under these conditions, one may suppose that the signal from the photomultiplier will be a maximum only if the scattered radiation falls on it from equal layers in the liquid and gaseous phases. With the use of the intensity of light scattering averaged in this way at the height $H=0$, the singular components of second order in the susceptibility^[6] mutually cancel, and this gives rise to the possibility of investigating the power law behavior of $I(t)$ along a phase boundary.

According to Fisher,^[7] the connection between the intensity of the scattered radiation and the correlation range R_c of a medium can be expressed in the form

$$I(H, t) = \frac{C[R_c(H, t)]^{2-\eta}}{[1+k^2 R_c^2(H, t)]^{1-\eta/2}}, \quad (1)$$

C is a constant and $k = 4\pi n \lambda^{-1} \sin(\theta/2)$. At the critical point itself ($H=0$, $t=0$) the intensity of light scattering at an angle of 90° is finite:

$$I_{cr}(H=0, t=0) = C/k^{2-\eta}. \quad (2)$$

Solving Eq. (1) for R_c with (2) taken into account and neglecting in the argument of the exponential the quantity $\eta^2/2$ in comparison with 2, we have

$$R_c(H, t) = \frac{1}{k} \left\{ \left[\frac{I_{cr}}{I(H, t)} \right]^{1+\eta/2} - 1 \right\}^{-1/\eta}. \quad (3)$$

The critical exponent η was taken to be equal to 0.06 in accordance with numerical calculations based on the three-dimensional Ising model. This result is experimentally confirmed in^[8].

In the calculations of the field dependence of the correlation range by formula (3), the symmetrized values of the intensity of scattered light $I_{sm} = \frac{1}{2}[I(H>0) + I(H<0)]$ were used. The values $I(H>0)$ and $I(H<0)$ were taken at heights symmetric with respect to the level $H=0$. For the calculation of R_c according to (3), it was assumed in advance that $\eta=0.06$. As a consequence, the error in the determination of the correlation range is directly connected only with the indicated errors in the single-scattering intensity. Thus, the correlation range changes along a critical isotherm from $70 \pm 5 \text{ \AA}$ at a

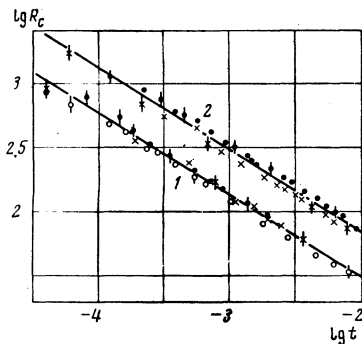


FIG. 1. The behavior of the correlation range on the critical isochor (2) and on the phase boundary (1): x— n -pentane, ●—solution of 26.8% benzene in n -pentane, ○—solution of 38.3% benzene in n -pentane.

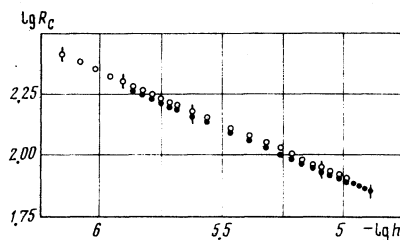


FIG. 2. Field dependence of the correlation range in n -pentane; ●— $\lambda_1 = 5461 \text{ \AA}$, ○— $\lambda_2 = 4358 \text{ \AA}$.

height $H=20 \text{ mm}$ to $250 \pm 20 \text{ \AA}$ at a height $H=1 \text{ mm}$.

According to scaling theory,^[9] the behavior of the correlation range along a critical isochor, a phase boundary, and a critical isotherm is described by power laws of the form

$$R_1 = r_1 |t|^{-1/\Delta_t}, \quad (4)$$

$$R_2 = r_2 |t|^{-1/\Delta_t}, \quad (5)$$

$$R_3 = r_3 h^{-1/\Delta_h}. \quad (6)$$

Here $h = p_{cr} g H / P_{cr}$, Δ_h and Δ_t are the dimensionalities of the field variables h and t ; and p_{cr} and P_{cr} are the critical density and critical pressure of the system. Since critical pressure of the n -pentane–benzene solution was not measured, the height $|H|$ was used instead of the field variable h . The results of the calculation of the temperature dependence of the correlation range for $T > T_{cr}$ and $T < T_{cr}$ are presented in Fig. 1.

Within the indicated range of errors of R_c , it is impossible to observe in the present study the difference between the behavior of the correlation properties of individual substances and binary solutions on account of the renormalization of the critical exponents.^[10] The behavior of the correlation range of n -pentane and of n -pentane–benzene solutions along a critical isochor can therefore be described by the single formula (4). Taking into account the scatter of the points over the various substances, we obtain for Eq. (4) the following parameters averaged over the different substances: $r_1 = (3.6 \pm 0.3) \text{ \AA}$ and $\Delta_t = 1.56 \pm 0.07$.

The behavior of R_c along a phase boundary is described for all investigated substances by formula (5) with the parameters $r_2 = (1.6 \pm 0.15) \text{ \AA}$ and $\Delta_t = 1.56 \pm 0.07$. The experimentally obtained results for r_1 , r_2 , and Δ_t , within the range of error of the experiment, agree with the corresponding published data (1) on the temperature dependence of the correlation range along a critical isochor and a phase boundary.

The height dependence of the correlation range is given in Figs. 2 and 3. It follows from these data that for n -pentane $r_3 = 0.76 \pm 0.07 \text{ \AA}$ and $\Delta_h = 2.45 \pm 0.15$; for the n -pentane–benzene solutions, $\Delta_h = 2.45 \pm 0.15$.

In view of published experimental data on the field dependence of R_c , it is convenient to compare the obtained data with the results of certain theoretical calculations.^[11, 12] According to the drop model of a liquid,^[11] the dimensionality of the field variable Δ_h ^[9] is con-

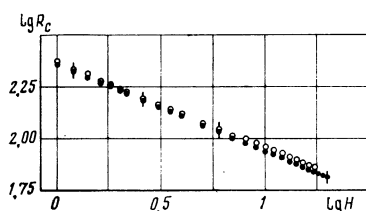


FIG. 3. Field dependences of the correlation ranges of the solutions: ●—26.8% benzene in *n*-pentane, ○—38.3% benzene in *n*-pentane ($\lambda = 5461 \text{ \AA}$).

ected with the critical parameters of a substance by the relationship

$$\frac{P_{cr}}{n_{cr} k_B T_{cr}} = \frac{\zeta(3-(2-\eta)/\Delta_h)}{\zeta(2-(2-\eta)/\Delta_h)} \quad (7)$$

where n_{cr} is the number of molecules in a unit volume at $h=0$, and $\zeta(\eta, \Delta_h)$ is the Riemann zeta function.^[13] Using the critical parameters of *n*-pentane^[14] and $\eta = 0.06$, we find that $\Delta_h = 2.49$.

The use of the ε -expansion method^[9,12] to calculate the critical exponents yields the following expression for the dimensionality of the field variable:

$$\Delta_h = \left[2 - \frac{n+2}{2(n+8)^2} \varepsilon^2 \right] \left\{ 3 + \varepsilon + \left[\frac{1}{2} - \frac{n+2}{(n+8)^2} \right] \varepsilon^2 \right\} \times \left\{ 2 + \varepsilon + \left[\frac{1}{2} - \frac{n+2}{(n+8)^2} \right] \varepsilon^2 \right\}^{-1} \quad (8)$$

According to (8), $\Delta_h = 2.56$ for $n=1$ and $\varepsilon=1$.

Within the limits of experimental error, the experimentally obtained quantity $\Delta_h = 2.45 \pm 0.15$ agrees with the presented theoretical calculations. Since the difference in the theoretical results is less than the experimental errors indicated above, it is impossible to give preference to either theoretical calculation on the basis of the data of the present experiment.

- ¹V. Puglielle and N. Ford, Phys. Rev. Lett. 25, 143 (1970).
- M. Giglio and G. W. Benedek, Phys. Rev. Lett. 23, 1145 (1971).
- S. Kagoshima, K. Ohbayashi, and A. Ikushima, Phys. Lett. 41A, 463 (1972).
- C. C. Lai and S. H. Chen, Phys. Lett. 41A, 259 (1972).
- J. S. Lin and P. W. Schmidt, Phys. Rev. Lett. 33, 1265 (1973).
- ²A. Z. Golik, A. D. Alekhin, N. P. Krupskii, A. V. Chalyi, and Yu. I. Shimanskiĭ, Ukr. Fiz. Zh. 14, 475 (1969).
- ³A. D. Alekhin and N. P. Krupskii, Pis'ma Zh. Eksp. Teor. Fiz. 14, 581 (1971) [JETP Lett. 14, 403 (1971)].
- ⁴A. D. Alekhin and N. P. Krupskii, in: Fizika zhidkogo sostoyaniya (Physics of the Liquid State), Kiev State Univ. Press, 3, 48 (1975).
- ⁵A. V. Chalyi and A. D. Alekhin, Zh. Eksp. Teor. Fiz. 59, 337 (1970) [Sov. Phys. JETP 32, 181 (1971)].
- ⁶B. Widom and F. H. Stellinger, J. Chem. Phys. 58, 616 (1973).
- J. J. Rehr and N. D. Mermin, Phys. Rev. A8, 472 (1973).
- F. J. Wegner, Phys. Rev. B5, 4529 (1972).
- A. V. Chalyi, Ukr. Fiz. Zh. 18, 1878 (1973).
- ⁷M. E. Fisher, J. Math. Phys. 5, 944 (1964).
- ⁸M. A. Anisimov, A. M. Yevtyushenko, Yu. F. Kiyachenko, and N. K. Yudin, Pis'ma Zh. Eksp. Teor. Fiz. 20, 378 (1974) [JETP Lett. 20, 170 (1974)].
- ⁹A. Z. Patashinskiĭ and B. L. Pokrovskii, Fluktuatsionnaya teoriya fazovykh perekhodov (Fluctuation Theory of Phase Transitions), Nauka, 1975.
- ¹⁰M. E. Fisher, Phys. Rev. 176, 257 (1968).
- M. A. Anisimov, A. V. Voronel' and E. E. Gorodetskiĭ, Zh. Eksp. Teor. Fiz. 60, 1117 (1971) [Sov. Phys. JETP 33, 605 (1971)].
- ¹¹F. Dyson, E. Montroll, M. Katz, and M. Fisher, Stability and Phase Transitions (Russ. Transl.), Mir, 1973, p. 297.
- ¹²K. Wilson, Phys. Rev. Lett. 28, 548 (1972).
- ¹³E. Jahnke, F. Emde, and F. Lösch, Tables of Higher Functions, McGraw-Hill, 1960 (Russ. Transl., Nauka, 1968, p. 88).
- ¹⁴N. B. Vargaftik, Spravochnik po teplofizicheskim svoĭstvam gazov i zhidkostiĭ (Handbook of the Thermophysical Properties of Gases and Liquids), Nauka, 1972.

Translated by S. J. Morin

Measurements of the yield point of crystalline He⁴

V. L. Tsymbalenko

Institute of Physical Problems, USSR Academy of Sciences

(Submitted October 5, 1976)

Zh. Eksp. Teor. Fiz. 72, 1885-1890 (May 1977)

Measurements are reported of the yield point of crystalline He⁴ at temperatures between 1.2 and 2.6 K and at pressures between 32 and 60 atm. It is found that the plastic properties of crystals with molar volumes of 19.1-20.6 cm³ are similar and resemble those of solid inert gases.

PACS numbers: 67.80.-s, 62.20.Fe

The amplitude of the zero-point oscillations in a solid constitutes a significant fraction of the interatomic distance. Therefore, quantum effects can make an appreciable contribution to the properties of crystalline helium, in particular, to its mechanical properties. As has already been shown in Refs. 1 and 2, delocalization of point vacancy defects can lead to unusual plastic

properties of the helium crystal, for example, to an anomalously low yield point, due to the high mobility of the delocalized point vacancy defects. In Refs. 2-5, no contribution of the vacancies of plastic flow was observed, and the conclusion was drawn that the motion of the dislocations was the main mechanism of plastic deformation. Plastic flow of helium polycrystals was

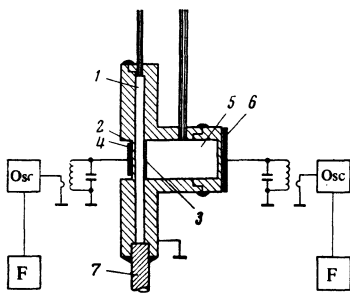


FIG. 1. Construction of the ampoule: 1—He⁴ crystal; 2—membrane of the pressure pickup at the crystal; 3—membrane of the pressure pickup at the pressure chamber; 4—plate of the capacitive pickup at the crystal; 5—pressure chamber; 6—plate of the capacitive pickup in the pressure chamber; 7—copper cold conductor.

studied in Ref. 4 in the case of large stresses and strains. The yield point can be estimated from the results of Ref. 4, and its temperature dependence can be determined. No effects of hydrostatic pressure on the plastic properties were observed in Ref. 4.

In the present work, the yield point was determined by measuring the residual stress after local deformation of the crystal. The ampoule shown in Fig. 1 was constructed for this purpose. The walls of the container were made of stainless steel of thickness 2 mm. A crystal of He⁴ was grown in the form of a disk of thickness 1 mm and diameter 22 mm in the volume 1. The growth of the crystal was initiated with a cold point—the copper cold conductor 7—and took place at constant pressure in a temperature gradient with rates of 5–10 μ/sec. Two identical membranes 2 and 3, of thickness 0.3 mm and diameter 6 mm were placed along the axis of the container. The membrane 2 with the plate 4 formed a capacitive pressure pickup connected in the tank circuit of a high-stability oscillator (osc), the frequency of which was measured by an electronic frequency meter (F) and recorded by an automatic recorder. A similar circuit was used for measurement of the pressure in the chamber 5. The stability of the oscillators, of the circuit parameters, and of the pickups made it possible to measure the pressure at the crystal with an accuracy of $\sim 3 \times 10^{-3}$ atm and in the chamber 5 with an accuracy to $\sim 10^{-2}$ atm. The temperature at the time of the experiment was maintained to within ~ 0.01 K. The local deformation of the crystal was achieved by motion of the membrane 3 as a result of a change in the pressure of the liquid helium located on the other side of this membrane in the special chamber 5. The deformation of the membrane was directly proportional to the difference between the pressure on the crystal and the pressure in the chamber 5. In all the measurements, the pressures in chamber 5 exceeded the corresponding change in pressure on the crystal by a factor of 30–200, so that we could assume, to within $\sim 3\%$, that the deformation of the membrane was determined only by the pressure in chamber 5. The profile of the membrane $z(r)$ is given by the formula $z(r) = ap_c(R^2 - r^2)^2$,^[6] where a is a constant coefficient that depends on the thickness, diameter, and Young's modulus

of the membrane, p_c is the pressure in the chamber, R is the outside radius of the membrane, and r is the distance from the axis of the membrane. A change in pressure in chamber 5 by 25 atm led to a $\sim 5 \mu$ motion of the center of the membrane, corresponding to a change $\Delta V_{\max} \cong 4 \times 10^{-5}$ cm³ in the volume of the crystal.

Upon change in the pressure in chamber 5, the membrane is deformed and deforms the helium crystal. This process can be divided into three stages: in the first stage the deformation takes place within the elastic limit; in the second, plastic flow begins at the center of the container and, with further motion of the membrane, the boundary of the region of plastic flow moves to the edges of the crystal; in the third, the plastic flow takes place throughout the volume of the ampoule.

In the first stage, the residual pressure p , measured by the pickup 4, will be directly proportional to the motion of the membrane $p \sim z(0)E/h$, where $z(0)$ is the deflection of the membrane at the center, h is the thickness of the crystal, and E is the average Young's modulus calculated from the elastic constants^[7,8] (see Fig. 4 below, the dashed lines B). The transient time is determined in this case by the velocity of sound and its order of magnitude is $\sim 10^{-5}$ sec. In the second stage, both elastically and plastically deformed regions of the helium crystal exist. Numerical estimates of the dependence of p on the movement of the membrane are difficult to make in this case. The time of establishment of the pressure p will be determined by processes of plastic flow of the solid helium. In the third stage, when the plastic flow of the helium takes place throughout the entire volume of the ampoule, we can propose a simple model.

Figure 2 shows the forces acting on the helium volume 3 inside the ampoule. Neglecting the dependence of p_r on z , the conditions of equilibrium of the solid helium can be written in the form

$$h \delta p_r / \delta r = 2N, \quad (1)$$

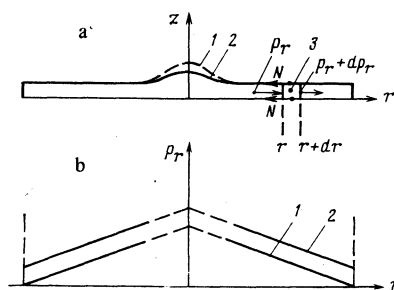


FIG. 2. a) Deformation of the crystal upon increase in the pressure in the chamber 5. The dashed line 1 is the initial position of the membrane, the solid line 2 is the final position. The profile of the membrane is not shown to scale. For the derivation of the equilibrium condition (1), the forces are shown acting on the volume 3; N is the shear stress on the surface of the crystal, p_r is the stress along the r axis; b) distribution of the stress p_r over the radius in the case in which plastic flow extends to the boundary of the container—curve 1. Curve 2 is the plot of p_r against r upon further deformation

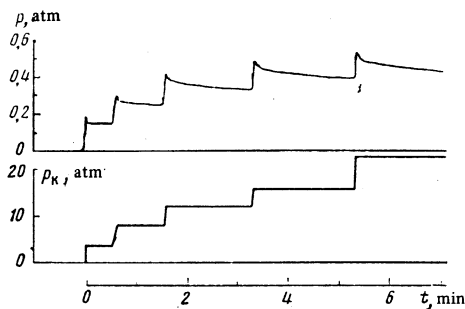


FIG. 3. Typical experimental plots of the pickup readings in the chamber and at the crystal. The lower curve is the stepwise change in the pressure in chamber 5. The upper curve is the corresponding change in the pressure at the crystal. The steps in the plots are due to apparatus effects (reading time of the frequency meter).

where N is the shear stress, equal to the yield point. The change in the volume of the crystal ΔV is connected with the change in the hydrostatic pressure Δp_0 at each point by the relation

$$\Delta V = K \int \Delta p_0(r) dV, \quad (2)$$

where K is the coefficient of hydrostatic compression, calculated from the elastic constants of the solid helium.^[7,8] In the plastically deformed crystal, the stress along any axis differs from the hydrostatic pressure by no more than the shear modulus, which is much smaller than p_0 . Therefore, the stress p_r can be equated to p_0 with little error and Eq. (2) can be integrated. After simplification, we obtain

$$\Delta p_0(0) = \frac{4NR_0}{3h} + \frac{\Delta V}{V_0K}, \quad (3)$$

where R_0 is the radius of the ampoule, V_0 is the total volume of the crystal, and $\Delta p_0(0)$ is the change in the hydrostatic pressure at the center of the crystal. It is seen from (3) that the pressure in the third stage will depend linearly on the deformation. The slope of this straight line is equal to the slope of the line of hydrostatic compression of the entire crystal (see Fig. 4 below, dashed lines A), and the constant term is proportional to the yield point.

The measurements were made on crystals grown at pressures 31, 41, 59 atm (the molar volumes were respectively 20.55, 20.12 and 19.14 cm³). For measurement of the plasticity limit in the increase in volume, the crystal was grown at a pressure of 25 atm in chamber 5. Then the pressure was reduced stepwise, in which case a short-time increase in temperature of the crystal by 0.01–0.03 K took place. Similar measurements of the yield point with decreasing volume were made by increasing stepwise the pressure in chamber 5 after the completion of growth of the crystal. The temperature of the crystal decreased in this case, within a short time ~5–10 sec, by 0.01–0.03 K. The linear rates of deformation of the solid helium along the z axis did not exceed $\sim 10^{-4}$ cm/sec and usually amounted to $(1-5) \times 10^{-5}$ cm/sec. For an estimate of the effect of the

deformation rate on the residual stress, several experiments were carried out at rates $\sim 3 \times 10^{-6}$ cm/sec. Within the limits of error, the results obtained at all rates were the same.

Synchronous plots of the readings of the pickups at the chamber (lower curve) and at the crystal (upper curve) are shown in Fig. 3. It is seen that the pressure change in chamber 5 leads to a change in the pressure at the pickup on the opposite side of the crystal, but with passage of time, the stresses decrease, i.e., they relax, without, however, decreasing to a value corresponding to the bulk compressibility of the entire crystal (Figs. 4a and 4b, dashed lines A). The main relaxation occurs within a time ~30–200 sec; during the subsequent time (on the order of one hour) the residual stress falls off by no more than 20% of the value of the previous relaxation. More prolonged measurements of the dependence of the residual stress on the time could not be carried out, since the rate of relaxation became comparable with the value of the drift of the measuring circuit. The total error in the determination of the residual stress was $\sim 15\%$.

The dependence of the residual stress on the deformation is nonlinear and is shown in Fig. 4a and 4b for two molar volumes. The maximum relative deformation of the crystal $\epsilon = z(0)/h$ is marked on the horizontal axis and the residual pressure p , measured by the pickup, on the vertical axis. The plus sign corresponds to an increase in the volume of the crystal, the minus to a decrease. Each curve is the result of averaging over two to four experiments, which were carried out in the following fashion. The arithmetic mean value $\langle p \rangle$ of the residual stresses p_i at maximum deformation and the experimental values at smaller deformations were multiplied by the ratio $\langle p \rangle / p$. At the beginning and the end of the curve is shown the calculated mean square error. The continuous curves are the result of reduction of the data on a high-speed computer by the method of least squares. It is seen in Fig. 4 that at high temperatures, the slope of the $p(\epsilon)$ curve decreases and becomes comparable (within the limits of error) with the slope of the straight line corresponding to the volume expansion of

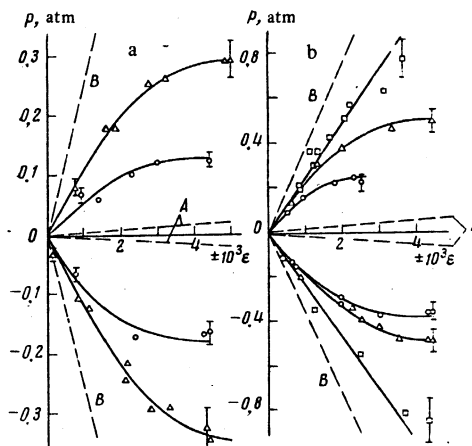


FIG. 4. Dependences of the residual stress on the deformation for two molar volumes: a— $V=20.55$ cm³, \circ — $T=1.68$ K, \triangle — $T=1.48$ K; b— $V=19.14$ cm³, \circ — $T=2.25$ K, \triangle — $T=1.78$ K, \square — $T=1.23$ K.

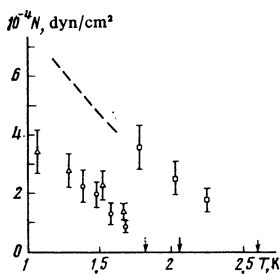


FIG. 5. Dependence of the plastic limit N on the temperature for the three molar volumes: \circ — $p=31$ atm, \triangle — $p=41$ atm, \square — $p=59$ atm. The arrows show the melting temperatures of the corresponding crystals. The dashed line is the lower limit of the yield point for crystals grown at 59 atm.

the crystal as a whole (the dashed lines in Fig. 4a and 4b). With decrease in temperature, the residual stress increases and there is no significant decrease in the slope for the crystal grown at a pressure of 59 atm. The $p(\epsilon)$ dependences obtained in compression and dilatation are identical. An exception is the $p(\epsilon)$ curve for the crystal grown at $p=59$ atm and $T=2.25$ K. Possibly, the reason is the small number of experiments.

The results reduced in accord with Eq. (3) are shown in Fig. 5 for three molar volumes. In the experiment, the actually measured quantity was the mean value of $p_x(0)$ but, in accord with what was said above, we can equate $p_0(0)$ with $p_x(0)$ with small error. Estimate gives $N/\Delta p_0 \sim 6 \times 10^{-2}$ for the yield point from the obtained data. This justifies the assumption made in the derivation of (3). It is seen that the yield point increases with decrease in temperature at all the molar volumes, according to a linear law and with identical slopes, within the limits of error. Similar dependences are characteristic of ordinary materials, and, in particular, for solidified inert gases.^{19]} The absolute values of the yield point, $N=(8-35) \times 10^4$ dyn/cm², agree with the values which can be obtained from Ref. 4. The effect of the density of solid helium on the yield point can also be seen from Fig. 5; this was not observed in Ref. 4. For a quantitative comparison of the plastic properties of

solid inert gases with crystalline helium, we use the ratio of the yield point to the coefficient of hydrostatic compression. The plasticity limits of Ne, Kr, Xe at $T \sim 0.7 T_{\text{melt}}$ were obtained from Ref. 9, and the corresponding coefficients of hydrostatic compression χ_T from Ref. 10. For these gases, the product $N\chi_T$ lies in the range $N\chi_T=(3-32) \times 10^{-5}$; the same quantity for helium at $T \sim 0.7 T_{\text{melt}}$ is of the order of $(7-10) \times 10^{-5}$, i. e., it is of the same order of magnitude.

We can thus conclude that the plastic properties of solid helium in the measured temperature and pressure ranges are similar to the plastic properties of ordinary materials and in particular, similar to those of the other solid inert gases.

I express my gratitude to A. I. Shal'nikov for constant attention and direction of the research, and also to A. F. Andreev, L. P. Mezhev-Deglin and Yu. V. Sharvin for valued discussions of the results.

¹A. F. Andreev and I. M. Lifshitz, Zh. Eksp. Teor. Fiz. 56, 2057 (1969) [Sov. Phys. JETP 29, 1107 (1969)].

²A. E. Meierovich, Zh. Eksp. Teor. Fiz. 71, 1180 (1976) [Sov. Phys. JETP 44, 617 (1976)].

³A. Andreev, K. Keshishev, L. Mezhev-Deglin and A. Shal'nikov, Pis'ma Zh. Eksp. Teor. Fiz. 9, 507 (1969) [JETP Lett. 9, 306 (1969)].

⁴H. Suzuki, J. Phys. Soc. Japan 35, 1472 (1973).

⁵V. L. Tsymbalenko, Pis'ma Zh. Eksp. Teor. Fiz. 9, 507 (1969) [JETP Lett. 23, 653 (1976)].

⁶L. D. Landau and E. M. Lifshitz, Teoriya uprugosti (Theory of Elasticity) Nauka, 1965, p. 69 [Pergamon, 1971].

⁷D. S. Greywall, Phys. Rev. A3, 2106 (1971).

⁸J. P. Franck and R. Wanner, Phys. Rev. Lett. 25, 345 (1970).

⁹I. N. Krupskii, A. V. Leont'eva and Yu. S. Stroilov, Zh. Eksp. Teor. Fiz. 65, 1917 (1973) [Sov. Phys. JETP 38, 957 (1974)].

¹⁰P. A. Bezuglyi and L. M. Tarasenko, Fiz. Nizk. Temp. 1, 731 (1975) [Sov. J. Low Temp. Phys. 1, 352 (1975)].

Translated by R. T. Beyer